AGU ADVANCING EARTH AND SPACE SCIENCES

AGU Advances

RESEARCH ARTICLE
10.1029/2026AV002343

Peer Review The peer review history for this article is available as a PDF in the Supporting Information.

Key Points:

- Multipoint observations from MAVEN and Tianwen-1 reveal a potential link between magnetic reconnection and the magnetotail flapping at Mars
- Magnetotail current sheet (CS) flapping at Mars may be triggered by plasma instabilities driven by reconnection-generated magnetic flux ropes
- First multipoint investigation of the magnetotail CS flapping mechanism beyond Earth

Supporting Information:

Supporting Information may be found in the online version of this article.

Correspondence to:

Y. Wen,
yuanzheng-wen@uiowa.edu

Citation:

Wen, Y., Halekas, J. S., Shen, H.-W., Zhang, C., Lillis, R. J., Gao, J., et al. (2026). Magnetic reconnection as a potential trigger for magnetotail flapping at Mars: Insights from MAVEN and Tianwen-1 observations. *AGU Advances*, *7*, e2026AV002343. https://doi.org/10.1029/2026AV002343

Received 10 FEB 2026
Accepted 19 MAR 2026

Author Contributions:

Conceptualization: Yuanzheng Wen
Data curation: Jared R. Espley, David L. Mitchell, Christian Mazelle, James P. McFadden
Formal analysis: Yuanzheng Wen, Jasper S. Halekas
Funding acquisition: Jasper S. Halekas, Shannon M. Curry
Investigation: Yuanzheng Wen, Jasper S. Halekas

Magnetic Reconnection as a Potential Trigger for Magnetotail Flapping at Mars: Insights From MAVEN and Tianwen-1 Observations

Yuanzheng Wen[1], Jasper S. Halekas[1], Han-Wen Shen[1], Chi Zhang[2], Robert J. Lillis[3], Jiawei Gao[2], Norberto Romanelli[4,5], Long Cheng[6], Chuanfei Dong[2], Yingjuan Ma[7], Yaxue Dong[8], Shaosui Xu[3], David A. Brain[8], Junfeng Qin[3,8], Jared R. Espley[4], David L. Mitchell[3], Christian Mazelle[9], James P. McFadden[3], and Shannon M. Curry[8]

[1]Department of Physics and Astronomy, University of Iowa, Iowa City, IA, USA, [2]Department of Astronomy, Center for Space Physics, Boston University, Boston, MA, USA, [3]Space Sciences Laboratory, University of California, Berkeley, CA, USA, [4]NASA Goddard Space Flight Center, Greenbelt, MD, USA, [5]Department of Astronomy, University of Maryland, College Park, MD, USA, [6]Swedish Institute of Space Physics, Uppsala, Sweden, [7]Department of Earth, Planetary and Space Sciences, University of California, Los Angeles, CA, USA, [8]Labortary for Atmospheric and Space Physics, Boulder, CO, USA, [9]Institut de Recherche en Astrophysique et Planétologie (IRAP), Université de Toulouse, CNRS, CNES, OMP, Toulouse, France

Abstract Magnetotail current sheet (CS) flapping is a universal plasma phenomenon observed at multiple planets, yet its triggering mechanisms remain poorly understood outside of Earth. At Mars, single-spacecraft observations have also reported tail flapping, but the processes responsible for its onset have never been identified. In this study, we investigate the potential correlation between magnetic reconnection and magnetotail flapping using multipoint measurements from Mars Atmosphere and Volatile EvolutioN (MAVEN) and Tianwen-1 (TW-1) missions. We analyze an example event in which MAVEN observed a reconnection-associated CS crossing in the near tail while TW-1 simultaneously detected CS flapping further downtail. A statistical survey of joint observations from November 2021 to February 2024 identifies that about two-thirds of TW-1 flapping events coincide with reconnection signatures observed by MAVEN. Multiple magnetic flux ropes were also detected before or during flapping intervals, similar to previous observations at Earth, suggesting that reconnection-generated magnetic flux ropes may propagate tailward and drive plasma instabilities that trigger the tail flapping at Mars. These results provide the first multipoint evidence of a potential statistical correlation between magnetic reconnection and magnetotail flapping at Mars, enabling us to explore the potential triggering mechanism of magnetotail flapping. Our findings also offer new insights into Martian magnetotail dynamics and broaden the comparative understanding of this fundamental plasma process across planetary environments.

Plain Language Summary The solar wind, a continuous stream of charged particles from the Sun, interacts with planetary magnetic fields and atmospheres to form long magnetic tails behind planets. Within these tails, thin layers of electric current—called current sheets—sometimes move or "flap," affecting how magnetic energy and plasma are transported. At Earth, observations from multiple spacecraft have shown that magnetic reconnection, a process in which magnetic field lines break and reconnect to release stored magnetic energy, can drive such motions. At Mars, however, the causes of current sheet flapping at the magnetotail have remained uncertain because previous studies only relied on a single spacecraft measurement. In this study, we use simultaneous observations from NASA's MAVEN spacecraft and China's Tianwen-1 orbiter to explore what triggers flapping in Mars's magnetotail. The results suggest that magnetic reconnection may also play a key role in triggering these motions at Mars, providing the first multipoint evidence of this connection and advancing our understanding of the plasma dynamics within the magnetotail of Mars.

1. Introduction

Magnetotail current sheet (CS) flapping refers to the up and down, or back and forth motion of current sheets, typically observed by spacecraft as multiple CS crossings (Rong et al., 2010; Runov et al., 2009; Sergeev et al., 1998; Speiser & Ness, 1967; Tsutomu & Teruki, 1976). Such flapping motions can substantially alter the global magnetic configuration of the magnetosphere and contribute to energy transport within the magnetotail

Methodology: Yuanzheng Wen, Jasper S. Halekas, Han-Wen Shen, Chi Zhang, Jiawei Gao
Software: Yuanzheng Wen
Supervision: Jasper S. Halekas
Visualization: Yuanzheng Wen
Writing – original draft: Yuanzheng Wen
Writing – review & editing: Jasper S. Halekas, Han-Wen Shen, Chi Zhang, Robert J. Lillis, Jiawei Gao, Norberto Romanelli, Long Cheng, Chuanfei Dong, Yingjuan Ma, Yaxue Dong, Shaosui Xu, David A. Brain, Junfeng Qin

(Sitnov et al., 2014, 2019). At Earth, multi-point measurements from missions such as Cluster, THEMIS, and MMS have enabled separation of spatial and temporal variations, leading to extensive studies of CS flapping properties over the past several decades (Gabrielse et al., 2008; Gao et al., 2018; Petrenko et al., 2023; Rong et al., 2015b; Sergeev et al., 2004; T. Zhang et al., 2002, 2005). Although the exact triggering mechanism remains inconclusive, previous studies have highlighted several possible drivers, including variations in solar wind conditions (Forsyth et al., 2009; Sergeev et al., 2008; C. Shen et al., 2008; G. Wang et al., 2019), Kelvin-Helmholtz instabilities (Nakagawa & Nishida, 1989), magnetic double-gradient instabilities (Erkaev et al., 2007, 2008), internal ion–ion kink instability (Karimabadi et al., 2003), magnetic reconnection and its associated bursty bulk flows (Gabrielse et al., 2008; Hwang et al., 2026; Sergeev et al., 2006; Volwerk et al., 2004; Vörös, 2011; Wei et al., 2019; Wu et al., 2016; Y. Zhang et al., 2020). Beyond Earth, magnetotail CS flapping has been reported at Mercury (Poh et al., 2020; C. Zhang et al., 2020), Venus (Rong et al., 2015a), Mars (DiBraccio et al., 2017; C. Zhang et al., 2023), and the giant planets Jupiter and Saturn (Volwerk et al., 2013; Xu et al., 2025). However, at these planets, single-spacecraft measurements limit the ability to distinguish between spatial and temporal variations, making it impossible to directly identify the potential triggering mechanisms of this universal plasma process. As a result, the drivers of tail flapping beyond Earth remain largely unexplored.

Unlike Earth, Mars lacks a strong intrinsic magnetic field, making its interaction with the solar wind and the interplanetary magnetic field (IMF) fundamentally different (Bertucci et al., 2011; J. S. Halekas et al., 2021; Nagy et al., 2004). Induced currents in the ionosphere lead to the formation of a magnetic barrier, which provides the main obstacle to the solar wind flow. Mass loading by ionized atmospheric constituents further contributes to the slowing of the plasma flow and draping of the IMF (Azari et al., 2023; H.-W. Shen et al., 2025, 2026; Szegö et al., 2000). Consequently, a distinct magnetotail structure forms, consisting of two magnetic lobes separated by a central CS with antiparallel magnetic field lines on either side (Dubinin & Fraenz, 2015; J. Halekas et al., 2006; C. Zhang et al., 2022). The induced magnetotail is highly dynamic in terms of its position, structure, and plasma compositions (Li et al., 2023; Liemohn & Xu, 2018; Wen, Rong, et al., 2025; C. Zhang et al., 2024), and it serves as a critical channel for ion escape (Barabash et al., 2007, 2025; Dong et al., 2015, 2017; Dubinin et al., 2012; Nilsson et al., 2010, 2023; H.-W. Shen et al., 2024). Additionally, Mars has localized crustal magnetic fields (Acuna et al., 1999), particularly concentrated in the southern hemisphere, which adds further complexity to its magnetospheric structure and plasma dynamics in the magnetotail (Brain et al., 2003; DiBraccio et al., 2018, 2022; Dubinin et al., 2023; Ma et al., 2014).

Continuous observations from the Mars Atmosphere and Volatile EvolutioN (MAVEN) mission (Jakosky et al., 2015) over the past decade have substantially advanced our knowledge of plasma dynamics in the magnetotail of Mars. Previous studies have revealed tailward escape of suprathermal planetary ions through the tail CS (Dong et al., 2015, 2017; Harada et al., 2015b; Inui et al., 2019), the dynamic twisting and shift of the magnetotail CS structure (DiBraccio et al., 2018, 2022; Wen, Rong, et al., 2025), bulk plasma acceleration associated with the magnetic reconnection (Harada et al., 2015a, 2017, 2020; L. Wang et al., 2023; Wen, Halekas, et al., 2025), the formation and detachment of magnetic flux ropes (DiBraccio et al., 2015; Hara et al., 2015, 2017, 2022; L. Wang et al., 2022), and the flapping motion of the magnetotail CS (DiBraccio et al., 2017; C. Zhang et al., 2023). These discoveries demonstrate the complex and highly dynamic nature of Mars' induced magnetotail. Despite these advances, our current knowledge is also constrained by the single-spacecraft measurement of MAVEN, particularly regarding the complexity of the tail's magnetic field structure. Such observations cannot fully resolve the temporal and spatial evolution of transient phenomena like reconnection or establish causal connections between physical processes occurring in different regions of the magnetotail. In particular, the triggering mechanism of Martian CS flapping and its possible coupling with other physical processes remain poorly understood. Addressing these questions requires multipoint measurements capable of resolving both spatial and temporal variability, as has been achieved at Earth (Lillis et al., 2022; Sánchez-Cano et al., 2022).

In this study, we present the first coordinated observations of the Martian magnetotail using simultaneous observations from MAVEN and China's Tianwen-1 (TW-1) orbiter (Y. Zou et al., 2021), providing novel insights into plasma dynamics within the tail region. We identify a series of CS flapping events detected by TW-1 in the distant tail and investigate their potential connection to the magnetic reconnection observed by MAVEN in the upstream tail regions. By combining simultaneous observations from both upstream and downstream tail regions, we provide new insights into the possible coupling between magnetic reconnection-driven dynamics and magnetotail CS flapping motions, offering the first multipoint perspective on the potential triggering mechanism of magnetotail flapping beyond Earth.

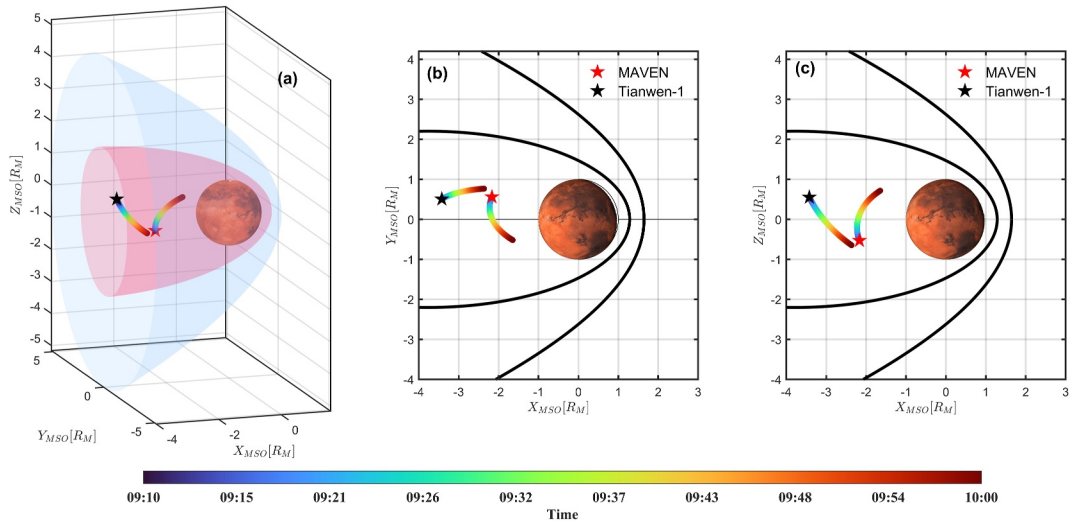

Figure 1. (a–c) MAVEN and Tianwen-1 trajectories in Mars Solar Orbital coordinates. The black curve represents the bow shock and induced magnetosphere boundary models based on Vignes et al. (2000).

2. Data Set and Instrumentation

The data used in this study are from the MAVEN and Tianwen-1 missions. Magnetic field measurements were made by both MAVEN and Tianwen-1. The Magnetometer (MAG) instrument (Connerney et al., 2015) onboard the MAVEN spacecraft provides three-dimensional magnetic field vector measurements with a cadence of up to 32 samples per second. Similarly, Tianwen-1's Mars Orbiter Magnetometer (MOMAG) instrument (Cheng et al., 2023, 2024, 2025; G. Wang et al., 2024; Y. Wang et al., 2023; Z. Zou et al., 2023) records magnetic field vectors at a sampling rate of 32 samples per second. The MAG and MOMAG data binned at a 1 s time resolution are used in this study. The Solar Wind Ion Analyzer utilizes an electrostatic analyzer consisting of two concentric near-hemispherical toroids, which provides three-dimensional distributions of ions in the energy range of 25 eV–25 keV, with a field of view (FOV) of 360° × 90°, and their moments data derived from this distribution at a time resolution of 4 s (J. Halekas et al., 2015, 2017). The MAVEN Solar Wind Electron Analyzer (SWEA) instrument provides electron energy spectrograms and pitch angle distribution at a temporal resolution of 2 s (D. Mitchell et al., 2016). The Suprathermal and Thermal Ion Composition (STATIC) instrument is equipped with an electrostatic top-hat analyzer and a time-of-flight velocity analyzer, allowing it to detect ions with energies ranging from 0.1 eV to 30 keV within a FOV of 360° × 90°. Its unique capabilities enable the identification of ion species according to their masses, with a cadence of 4 s (J. McFadden et al., 2015). Detailed ion (H^+, O^+, O_2^+) moments, including density and velocity, can be calculated from the corresponding three-dimensional particle distributions (Fowler et al., 2022).

3. Observations

3.1. A Case Study

We first present an example event jointly observed by MAVEN and TW-1 in the Martian magnetotail on 31 January 2024, as shown in Figure 1. During this interval, both spacecraft traversed the magnetotail, with MAVEN located in the near-tail region and TW-1 positioned farther downtail as shown in Figures 1a–1c. Figures 2a–2d show the three magnetic field components and the total field magnitude measured by the onboard magnetometers. Figures 2e–2g display the velocity moments of H^+, O^+, and O_2^+ derived from STATIC measurements, while Figures 2h and 2j–2l present the omnidirectional differential energy fluxes of electrons from SWEA and of ions from STATIC. A notable feature in this event is the reversal of the B_X component from negative to positive values (Figure 2a), accompanied by enhanced electron and ion fluxes together with ion energization. These signatures are characteristic of a CS crossing observed by MAVEN (Dubinin et al., 2012; J. Halekas et al., 2006; Wen, Rong, et al., 2025). Surprisingly, during the same time interval, TW-1 traversed the corresponding spatial region in the downstream tail from the opposite direction (Figure 1a). Unlike MAVEN, which recorded a typical single CS

10.1029/2026AV002343

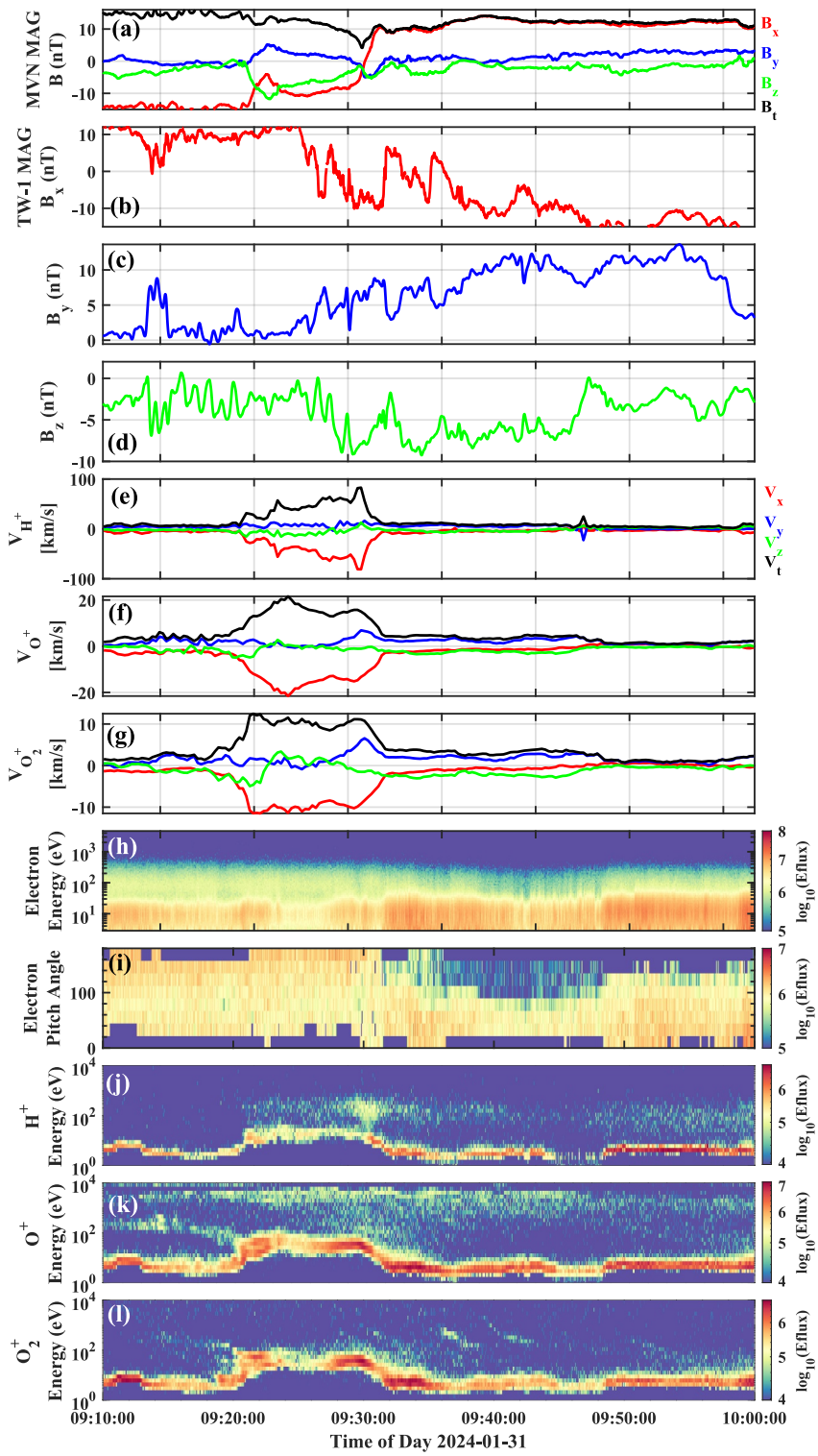

Figure 2. (a–d) MAVEN and Tianwen-1 magnetic field components in Mars Solar Orbital (MSO) coordinates. (e–g) Velocity components of H^+, O^+, and O_2^+ in MSO coordinates. (h) Electron energy and (i) pitch angle spectra from Solar Wind Electron Analyzer. (j–l) energy spectra of H^+, O^+, and O_2^+ ions.

crossing, TW-1 observed a transition from the $+B_X$ lobe to the $-B_X$ lobe with multiple CS crossings, as shown in Figure 2b. Such multiple CS crossings are commonly associated with the magnetotail CS flapping, as previously reported by DiBraccio et al. (2017) and C. Zhang et al. (2023). This raises an important question: why does MAVEN observe a single CS crossing in the near-tail region, while TW-1 detects multiple crossings—or flapping—in the same spatial sector farther downtail? To address this question, we next perform a detailed analysis of the observed CS crossings by MAVEN and TW-1.

3.1.1. Magnetic Reconnection Signatures

For MAVEN's CS crossing observations, we clearly identify a significant enhancement in tailward ion flows—particularly in H^+—together with a bipolar magnetic field signature across the crossing. In addition, the electron pitch angle distributions also display significant changes around the CS crossing (Figure 2i). Before the crossing, SWEA generally measured isotropic electron distributions, typical of draped magnetic field lines. After the crossing, the distribution changes into a one-sided loss cone distribution, indicating the presence of open field line structures (Brain et al., 2007). Such transitions in magnetic field topology are also strong indicators of magnetic reconnection. Taken together, these features provide potential evidence for reconnection (Eastwood et al., 2008; J. Halekas et al., 2009; Harada et al., 2015a; Wen, Halekas, et al., 2025). To provide more comprehensive evidence for the magnetic reconnection, we next examine additional plasma and field signatures for the CS crossing. We transformed both the magnetic field and ion velocity vectors from the Mars Solar Orbital (MSO) coordinate system into the local LMN coordinate system (L is along the antiparallel magnetic field direction, M is along the X line, and N is along the CS normal) for the time interval of 09:29:00 to 09:32:30 UT. The LMN coordinates over this interval were determined using the Minimum Variance Analysis (MVA) method (Sonnerup, 1998), which is a standard technique for determining the local CS geometry. The eigenvectors calculated from the MVA correspond to the following orientations in MSO coordinates: $L = [1.00, 0.033, 0.011], M = [0.034, -0.84, -0.54], N = [-0.0087, 0.54, -0.84]$. The reliability of the LMN transformation is confirmed by the eigenvalue ratios ($\lambda_1/\lambda_2 = 7.51$ and $\lambda_2/\lambda_3 = 19.48$) (Sonnerup, 1998; DiBraccio et al., 2015), ensuring accurate alignment for analyzing the reconnection region. As shown in Figure 3a, the magnetic field B_L component reversed polarity from negative to positive, while the B_M component exhibited a clear bipolar variation, transitioning from positive to negative. Meanwhile, the B_N component remained positive and relatively stable throughout the crossing. These signatures are characteristic of Hall magnetic fields, which are widely recognized as indicators of the ion diffusion region during collisionless magnetic reconnection (Eastwood et al., 2008; J. Halekas et al., 2009; Harada et al., 2017; Wen, Halekas, et al., 2025). Additionally, we observe a pronounced tailward enhancement of V_L for H^+ reaching ~80 km/s in Figure 3b, which represents a reconnection-driven ion jet (Harada et al., 2015a, 2020). In contrast, the velocities of heavy ions show only slight deviations (Figures 3c and 3d), as expected due to their unmagnetized behavior (Harada et al., 2017; Liu et al., 2015). Together, the magnetic field and plasma signatures are consistent with the features of a type-4 reconnection CS crossing, as categorized by Harada et al. (2017).

Lastly, we perform a qualitative Walén test to further confirm the occurrence of magnetic reconnection (Phan et al., 2004; Vörös et al., 2017; Wen, Halekas, et al., 2025; Y. Zhang, 2016). In theory, reconnection outflows are expected to accelerate to the local Alfvén speed (Parker, 1957), defined as $V_A = \frac{B}{\sqrt{\mu_0 \rho}}$, where B is the magnetic field and ρ is the total plasma mass density, including contributions from H^+, O^+, and O_2^+. The Walén test evaluates whether correlations exist between the Alfvén velocity ($\pm V_A$) and the plasma velocity in the de Hoffmann–Teller (HT) frame, $V - V_{HT}$, where V_{HT} is the HT velocity (De Hoffmann & Teller, 1950). The HT frame velocity can be estimated from a set of plasma bulk velocity measurements, $\mathbf{v}^m$, and magnetic field measurements, $\mathbf{B}^m$ ($m = 1, 2, \ldots, M$). Specifically, one seeks a reference frame in which the mean square of the convective electric field is minimized. This mean square is defined as

$$D(V) = \frac{1}{M} \sum_{m=1}^{M} |(v^m - V) \times B^m|^2.$$

The HT velocity, $\mathbf{V}_{HT}$, is then obtained as the value of $\mathbf{V}$ that minimizes $D(\mathbf{V})$ (Khrabrov & Sonnerup, 1998; Sonnerup et al., 1987). The $\pm$ signs correspond to outflows in the $\pm L$ directions, matching also the $\pm$ sign of the normal magnetic field B_N. Accordingly, in scatterplots of V_A versus $V - V_{HT}$, a strong linear correlation with a

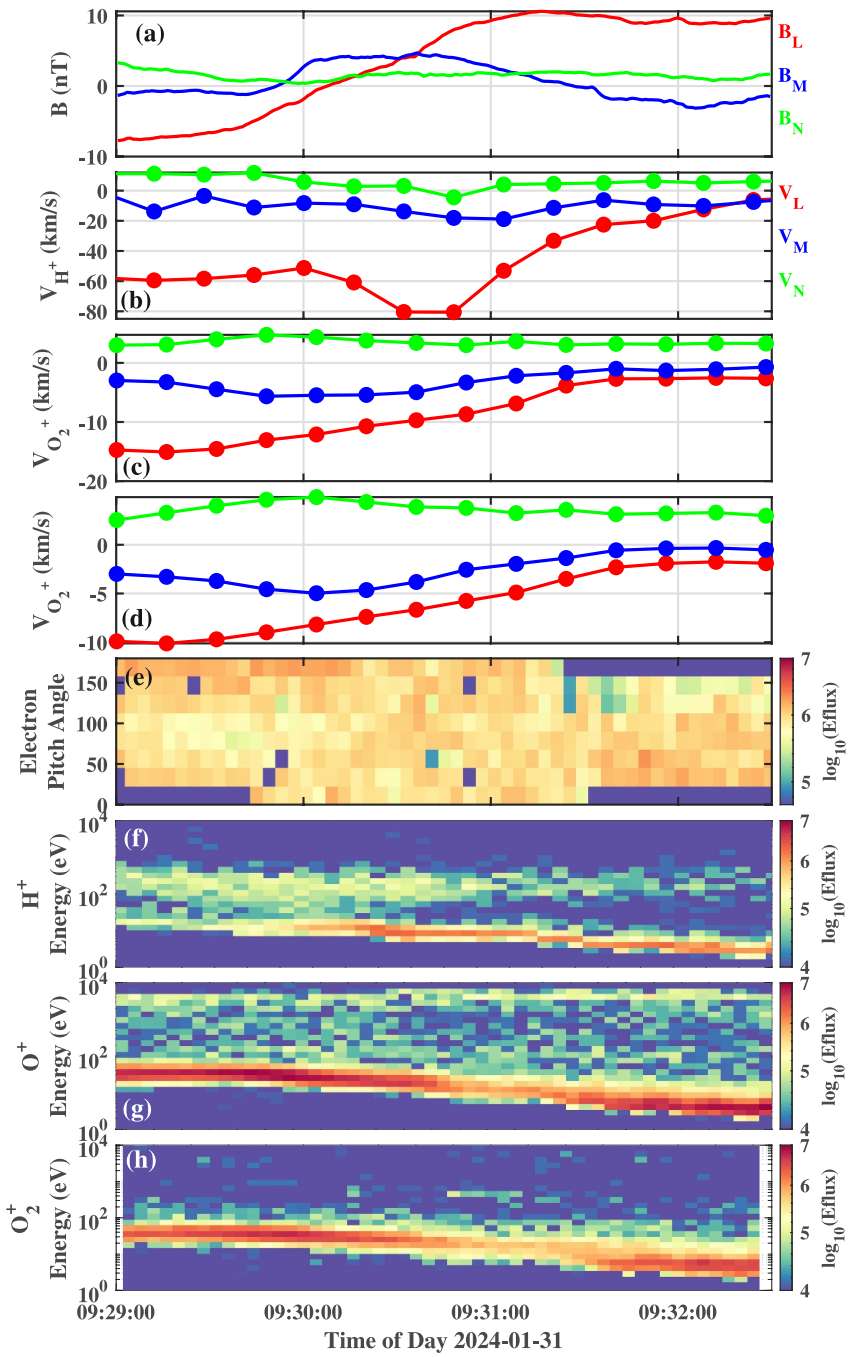

Figure 3. Zoom-in of the current sheet crossing by MAVEN on 31 January 2024 during 09:29:00–09:32:30 UT. (a) The three components of the magnetic field in LMN coordinates. (b–d) Velocity component H^+, O^+, and O_2^+ in LMN coordinates. (f) Electron pitch angle distributions (111–140 eV). (f–h) Energy spectrograms of H^+, O^+, and O_2^+.

regression slope near ±1 is expected within reconnection outflows (Paschmann & Sonnerup, 2008; Vörös et al., 2017; Wen, Halekas, et al., 2025; Y. Zhang, 2016). As shown in Figure 4, scatterplots of V_A versus $V - V_{HT}$ (with red, blue, and green points representing the three velocity components) are presented for the intervals 09:25:40–09:28:10 and 09:31:30–09:34:30, the two intervals were chosen to capture distinct outflow regions separated by the B_L reversal, ensuring each segment represents a quasi-steady flow (Vörös et al., 2017). Clear correlations are observed, with slopes consistent with the conditions required for the Walén test. A change in the sign of the slopes can be interpreted in two ways: (a) the spacecraft remained on the same side of the X-line

10.1029/2026AV002343

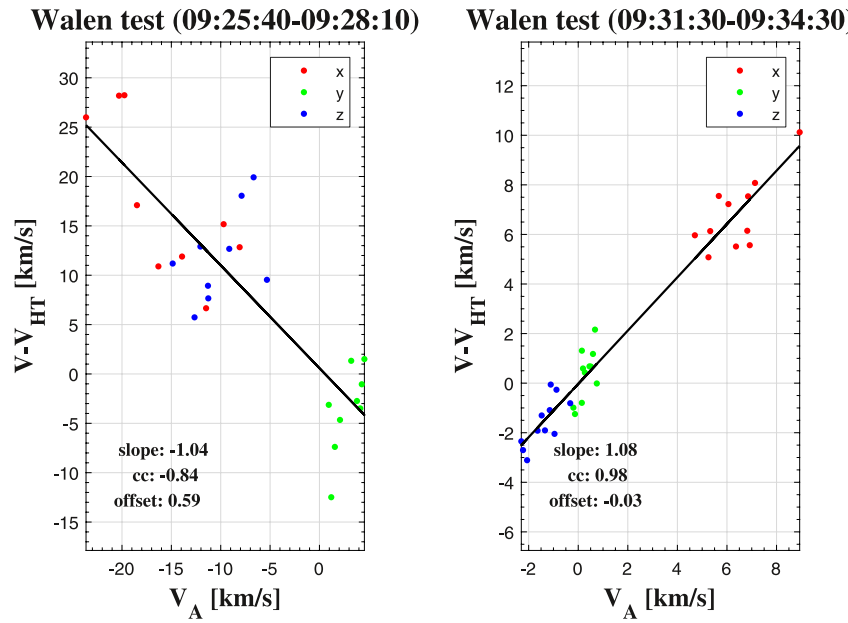

Figure 4. Walén relation test in the deHoffmann-Teller (HT) frame: comparisons between the observed ion velocities in HT frame and the Alfvén velocity. The three velocity components are indicated with color dots. The lines represent a linear regression fit of the outflows.

while crossing both boundaries of a single outflow, or (b) the spacecraft crossed to the opposite side of the X-line, sampling oppositely directed outflows within the same hemisphere (Øieroset et al., 2000; Vörös et al., 2017). Since the changes in regression slope are associated with reversals in B_L, we interpret these results as evidence that MAVEN crossed both sides of the reconnection X-line, consistent with the magnetic field and plasma signatures of a reconnection crossing as discussed above. All these signatures indicate that MAVEN likely observed the ion diffusion region of the magnetic reconnection.

3.1.2. Properties of the CS Flapping

As for the CS flapping observed by TW-1, our first step is to determine the flapping type using the method developed by Rong et al. (2015b), which has since been applied at multiple planets (DiBraccio et al., 2017; Rong et al., 2015a; Wu et al., 2016; Xu et al., 2025; C. Zhang et al., 2020). This technique relies on the temporal variation of the B_X component and the orientation of the CS normal. Once a multiple CS-crossing event is identified, the MVA is applied to the magnetic field data for each individual crossing to determine the CS normal direction $\hat{n}$ in both MSO and local coordinates (C. Zhang et al., 2023).

The key step of this method is calculating the so-called k-value for each crossing, defined as $k = \text{sign}(n_M \times n_N) \times \text{sign}(\Delta B_L)$, where "sign" denotes the sign function. For crossings where B_L changes from negative to positive ($-B_L$ to $+B_L$), $\Delta B_L > 0$ and the sign is positive. Conversely, for crossings where B_L changes from positive to negative ($+B_L$ to $-B_L$), $\Delta B_L < 0$ and the sign is negative. Applying this equation to a series of crossings yields a sequence of k values that characterizes the flapping type. An alternating pattern of $+1$ and -1 indicates steady flapping, whereas a sequence of k values that are consistently $+1$ or consistently -1 corresponds to kink-like flapping (DiBraccio et al., 2017; Rong et al., 2015b; C. Zhang et al., 2023). Table 1 summarizes the results of this CS analysis. For this flapping event, k stays at -1 always, confirming that the flapping motion belongs to kink-like flapping waves. It is also interesting to note that **n** is tilted in the y-z plane as shown by the larger values of n_y and n_z as compared to n_x, which is consistent with flapping waves observed at Earth and other planets (Poh et al., 2020; Rong et al., 2015a; Volwerk et al., 2013). Following this classification, we further apply the single-spacecraft technique developed by Rong et al. (2021) based on the MVA method and the Harris CS model, to estimate the physical properties of the CS flapping motion, including the propagation speed V_f, spatial amplitude A, and wavelength λ. Using the same approach as C. Zhang et al. (2023), we find that for the TW-1 event studied here, the propagation speed is $V_f \sim 8$ km/s, the spatial amplitude is $A \sim 259.5$ km, and the

Table 1
Minimum Variance Analysis on Martian Current Sheet Flapping Motion

Date	Time	Normal in MSO	λ_2/λ_3	k
2024-01-31	09:26:12–09:26:32	0.52, 0.62, 0.59	3.96	−1
	09:26:58–09:27:18	−0.26, −0.97, −0.035	31.40	−1
	09:27:35–09:28:04	0.20, −0.71, −0.67	4.49	−1
	09:31:33–09:31:50	−0.58, −0.54, 0.61	6.74	−1
	09:32:42–09:33:03	−0.035, −0.83, −0.55	3.52	−1
	09:33:57–09:34:46	0.39, 0.78, −0.50	7.93	−1
	09:35:02–09:35:14	−0.20, −0.81, 0.55	3.31	−1
	09:35:52–09:36:42	−0.0069, −0.78, −0.63	4.66	−1

wavelength is $\lambda \sim 1070$ km. It should be noted that, as discussed in Rong et al. (2021), this single-spacecraft method may carry uncertainties in estimating flapping wave parameters for individual crossings. However, it is still suitable for deriving representative average parameters over the full flapping interval.

Although a direct observational connection between the magnetic reconnection and the tail flapping may not be firmly established from two-point measurements, their correlation may still be examined indirectly from an energy perspective. Using the Sweet–Parker reconnection model (Parker, 1957; Sweet, 1958), we can estimate the energy flux released during reconnection in the Martian magnetotail. With lobe and normal magnetic field components of $|B_L| = 10$ nT and $|B_N| = 2$ nT, the reconnection rate is $R = |B_N|/|B_L| \sim 0.2$ (Gao et al., 2021; Guo et al., 2018), giving an inflow speed of $V_{in} \sim 16$ km/s. The resulting inflow energy flux is $\overrightarrow{W_{in}} = \left(\vec{E} \times \vec{H}\right)_{in} = V_{in}B_{in}^2/\mu_0 \approx 1.27 \times 10^{-6}$ W m^{-2}, while the outgoing flux is $W_{out} = \left(\vec{E} \times \vec{H}\right)_{out} = V_{out}B_{out}^2/\mu_0 \approx 2.55 \times 10^{-7}$ W m^{-2}. Thus, the net energy release is $W_{release} = W_{in} - W_{out} \approx 1.02 \times 10^{-6}$ W m^{-2}. Similarly, following the approach in C. Zhang et al. (2023), the magnetic energy flux carried by the flapping waves observed by TW-1 can be estimated as $W_f = \Delta B_L^2/2\mu_0 \times V_f \approx 0.3 \times 10^{-6}$ W m^{-2} based on parameters from our event. Although W_f is smaller than $W_{release}$, it is of the similar order of magnitude, suggesting that the reconnection-released energy is sufficient to account for the energy carried by the flapping waves. From the principle of energy conservation, this comparability provides indirect evidence for a potential correlation between reconnection and flapping, even in the absence of a direct observational link.

3.2. Statistical Survey and Results

Based on the above analysis for this event, although we have identified a potential spatial, temporal, and energy correlation between the magnetic reconnection observed by MAVEN and the CS flapping recorded by TW-1 in the downtail region, it remains challenging to make a direct observational link that would conclusively prove their coupling. Despite the fact that MAVEN and TW-1 follow completely different and independent trajectories and orbital periods, the large number of orbits (~4 years) available makes it possible to search for more joint-observation events like this. To explore this possibility, we further conducted a statistical survey to search for intervals where both spacecraft made observations of the close spatial regions within a short time window gap in the magnetotail of Mars, investigating whether a potential statistical correlation exists between magnetic reconnection occurrence and flapping events.

Specifically, we visually searched for MAVEN and TW-1 joint-observation events during the interval from November 2021 to February 2024, applying the following criteria: (a) both spacecraft must traverse the same or closely overlapping spatial regions of the magnetotail in the YZ plane in MSO coordinates; and (b) the temporal separation between the observations of two spacecraft should be less than 1 hr. Using these criteria, we initially identified 112 orbits that fulfilled the spatial and temporal constraints. However, because the detection of both reconnection and flapping events requires that the spacecraft cross the magnetotail CS, we further restricted our data set to cases where both MAVEN and TW-1 made clear CS crossings (B_x reversals), which reduced the sample to 59 orbits. From this reduced set, we first examined TW-1 data for CS flapping signatures and identified 34 tail flapping events (see Table S1 in Supporting Information S1). We then turned to MAVEN's CS crossings in the upstream tail regions to search for signatures of magnetic reconnection, following the procedure described in Harada et al. (2017). In this approach, we first visually inspected the magnetic field data for bipolar out-of-plane (B_M) signatures with high intermediate-to-minimum eigenvalue ratios ($\lambda_M/\lambda_N > 3$), and subsequently examined the ion velocity data to identify associated ion outflow jets. Using this method, we identified 22 events in which reconnection signatures were observed by MAVEN and flapping signatures were detected by TW-1. By contrast, 12 flapping events recorded by TW-1 did not show clear reconnection signatures in MAVEN data. Thus, roughly two-thirds of the identified tail flapping intervals appear to be associated with upstream reconnection, although this conclusion may be hampered given the limited statistics. To further assess potential bias in these statistics, we also searched for reconnection signatures in events without flapping. In this complementary survey, 23 events showed neither reconnection signatures by MAVEN nor flapping by TW-1, and only one case exhibited

Table 2
Contingency Table of Magnetic Reconnection (MAVEN) Versus Current Sheet Flapping (TW-1)

	Reconnection signatures	No reconnection signatures
CS flapping	22	12
No CS flapping	1	23

reconnection signatures in the upstream tail without corresponding flapping signatures in the downstream tail. However, in that single case, the observational gap between the two spacecraft far exceeded 1 hr, introducing the possibility of significant temporal variations that could obscure any causal relationship. These results can be summarized in a contingency table (Table 2).

We then applied statistical tests to evaluate the significance of this association. A chi-square test yielded $\chi^2 = 21.55$ with a p-value of 3.5×10^{-6}. The p-value represents the probability of obtaining the observed correlation (or a stronger one) if magnetic reconnection and tail flapping were in fact unrelated. Such a small p-value strongly rejects the null hypothesis of independence between the two processes (Greenwood & Nikulin, 1996). Fisher's exact test and Boschloo's test gave nearly identical results ($p \approx 1.8 \times 10^{-6}$), confirming that the observed correlation between magnetic reconnection and tail flapping is highly significant. To provide a more physically interpretable measure of this association, we further evaluated the conditional probabilities and odds ratio implied by the contingency table (Table 2). When upstream reconnection signatures are observed by MAVEN, the probability of downstream CS flapping observed by TW-1 is $22/(22 + 1) \approx 96\%$. In contrast, when reconnection signatures are absent, the probability of observing flapping is $12/(12 + 23) \approx 34\%$. The corresponding odds ratio is approximately $(22/1)/(12/23) \approx 42$, indicating that the occurrence of downstream flapping is more than an order of magnitude more likely when upstream reconnection signatures are present. However, it should be noted that these statistical results may not, by themselves, establish a direct causal relationship between magnetic reconnection and CS flapping. Instead, they demonstrate a robust statistical correlation and indicate that magnetic reconnection substantially increases the likelihood of downstream flapping under comparable spatial and temporal conditions.

Our statistical survey, therefore, indicates that about two-thirds of the CS flapping events observed by TW-1 in the downstream tail were accompanied by magnetic reconnection signatures detected by MAVEN in the upstream tail. This provides statistical evidence that magnetic reconnection is statistically intercorrelated with the tail flapping and may be a potential driving factor of CS flapping motions in the Martian magnetotail.

4. Discussion

Based on the analysis of the example event and a statistical survey of MAVEN and TW-1 joint observations in the magnetotail, we find a possible tendency for CS flapping observed by TW-1 in the distant magnetotail to occur preferentially when MAVEN detects magnetic reconnection in the near tail within the same spatial sector. Further supporting this scenario, previous work by DiBraccio et al. (2017) has shown that Martian magnetotail CS flapping occurs more frequently in the southern hemisphere in MSE coordinates, also consistent with the spatial distributions of magnetic reconnection reported by Harada et al. (2017) and L. Wang et al. (2023). Taken together, these findings suggest a possible correlation between the CS flapping and magnetic reconnection in the Martian magnetotail. In this section, we aim to provide a potential physical interpretation of how magnetic reconnection observed in the upstream tail may act as a trigger for the CS flapping in the downstream magnetotail.

Previous studies on Earth have extensively investigated how magnetic reconnection may trigger terrestrial magnetotail flapping. For instance, Wu et al. (2016) analyzed THEMIS observations and showed that flapping motions in the tailward reconnection outflow were closely associated with a magnetic flux rope, with the subsequent anisotropic ion flows in the post-flux-rope CS driving plasma instability that produced the flapping in the downstream tail. Similarly, Y. Zhang et al. (2020) reported a tail flapping event observed by Cluster tailward of a reconnection site detected by TC-1, where the reconnection-modified downstream plasma conditions appeared to facilitate plasma instability, leading to the flapping motion of the CS. These observational studies suggest that reconnection and its associated flux ropes can serve as triggers for tail flapping. Interestingly, magnetic flux rope signatures were also observed in our observations during the tail flapping events. Figure 5 shows an example magnetic flux rope event observed during a MAVEN and TW-1 joint interval. In this case, MAVEN detected a single CS crossing in the near tail regions, while TW-1 encountered CS flapping further downtail. Notably, before the encounter of flapping, TW-1 detected a magnetic flux rope structure around 16:45 (shaded regions) in Figure 5c. The converted vector magnetic fields in LMN coordinates (Figure 5f) exhibit a bipolar signature in the maximum variance (L) direction and a unimodal signature in the intermediate variance (M) direction. The hodograms show a smooth rotation in the L–M plane (Figure 5g) and a thin structure in the L–N plane (Figure 5h),

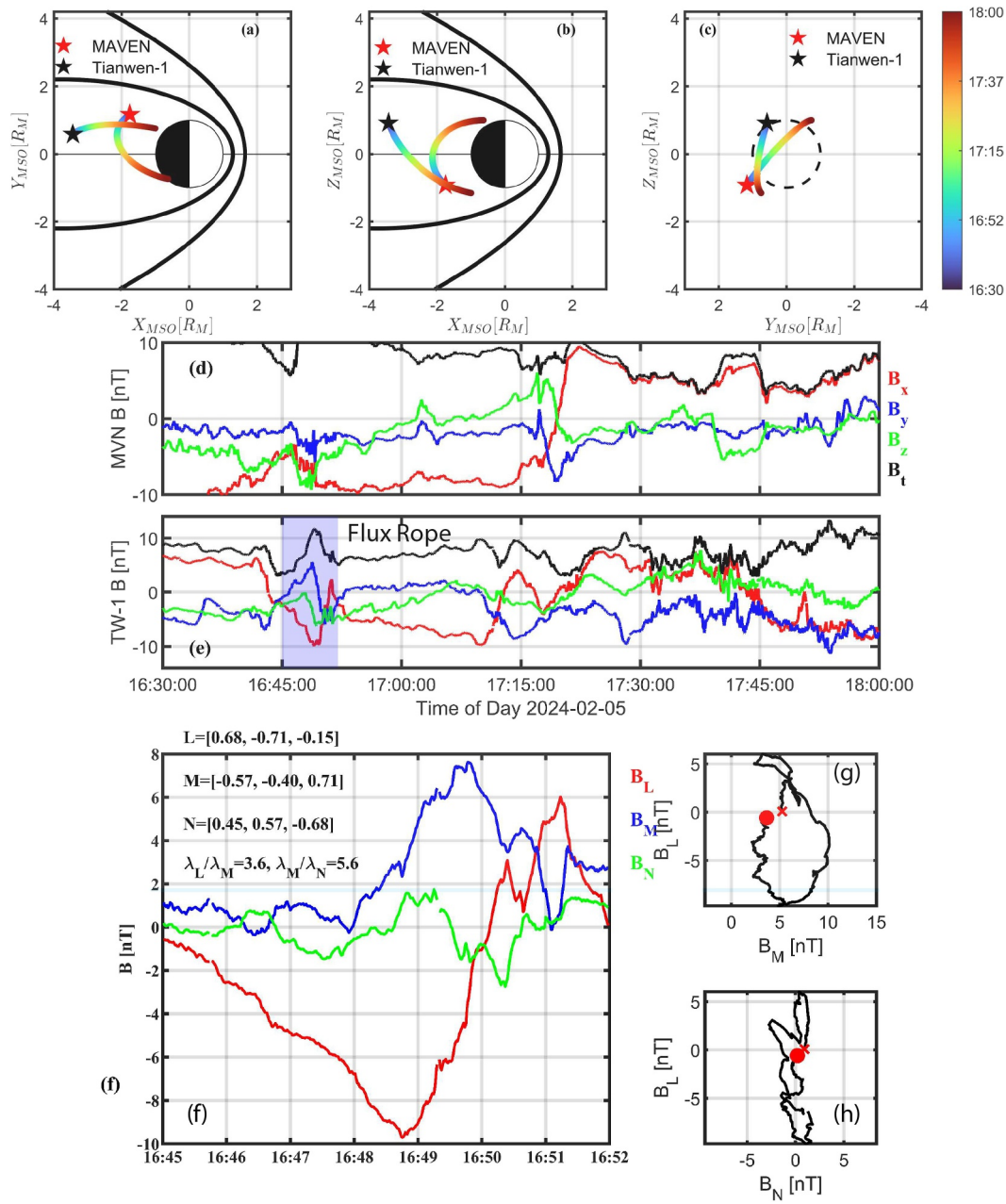

Figure 5. Overview of a magnetic flux rope observed during the flapping interval of a MAVEN and TW-1 joint observation. (a–c) The spacecraft trajectory projected onto the X-Y (left: Equatorial), X-Z (center: Meridian), Y-Z (right: Viewed from the Sun) planes in the Mars-centered Solar Orbital (Mars Solar Orbital (MSO)) coordinates, respectively. (d)–(e): magnitude and vector components of the magnetic field in the MSO coordinates. Flux rope observation interval is shaded. (f): The closed-up time series plots of the magnetic field structure during the flux rope encounter in LMN coordinates. Hodograms during the flux rope encounter corresponding to the time segment between two magenta dashed vertical lines are shown in (g) the Minimum Variance Analysis maximum-intermediate (L–M), and (h) maximum-minimum (L–N) planes.

consistent with characteristic magnetic flux rope signatures (Hara et al., 2017, 2022; Russell & Elphic, 1979). In our multipoint observations of the Martian flapping magnetotail, we have identified multiple magnetic flux ropes events (see Supporting Information S1), either observed by MAVEN in the upstream tail or by Tianwen-1 in the downstream tail, often appearing before or during intervals of CS flapping. Moreover, a previous study by Hara et al. (2022) also showed that magnetic flux ropes occur more frequently in the $-E$ hemisphere in MSE coordinates, also consistent with the spatial distribution of the tail flapping reported by DiBraccio et al. (2017). This

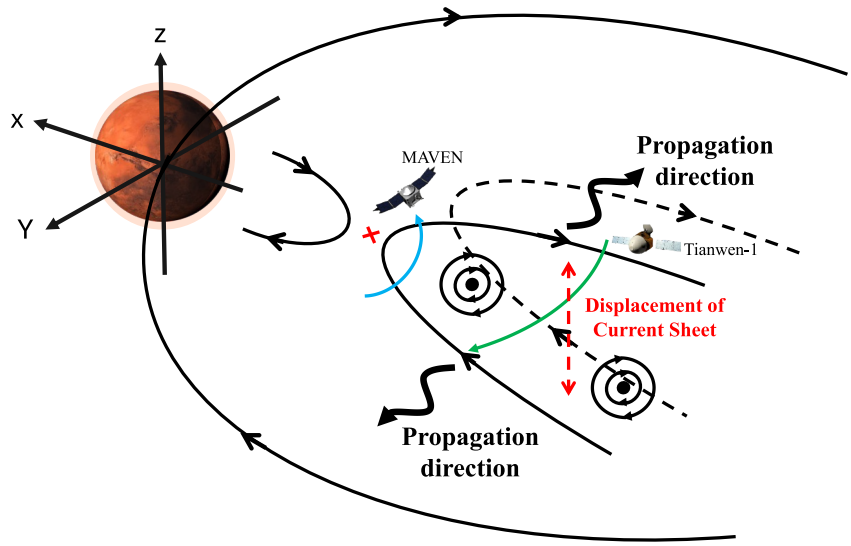

Figure 6. Schematic illustration of how magnetic reconnection potentially triggers the downstream tail current sheet (CS) flapping at Mars. MAVEN observes magnetic reconnection in the Martian magnetotail, which generates a chain of magnetic flux ropes that travel downstream and perturb the tail plasma. These perturbations, through plasma instabilities, drive flapping motions of the CS (indicated by red thick lines), subsequently observed by Tianwen-1. Crustal magnetic fields are omitted for clarity.

spatial and temporal association, suggested by previous studies and our observations, indicates that reconnection-generated magnetic flux ropes may play a potential role in controlling CS dynamics at Mars. Based on these observations, we propose a possible physical explanation for how magnetotail CS flapping may be triggered by magnetic reconnection in the Martian magnetotail. When magnetic reconnection is initiated (MAVEN observed the ion diffusion region during the crossing), a sequence of magnetic flux ropes is generated (Eastwood & Kiehas, 2015; Eastwood et al., 2012; Hara et al., 2017). As these magnetic flux ropes continuously propagate downtail, they may alter the plasma environment and drive plasma instabilities in the downstream magnetotail. Such instabilities driven by magnetic flux ropes could then account for the CS flapping observed by Tianwen-1 tailward of the magnetic reconnection site detected by MAVEN, perhaps in ways analogous to mechanisms inferred at Earth (Wu et al., 2016; Y. Zhang et al., 2020). Figure 6 illustrates a possible configuration of this dynamic process observed by MAVEN and TW-1 in the Martian magnetotail based on our argument.

In addition to multipoint observations, previous simulation studies have also highlighted links between magnetic reconnection and magnetotail flapping motions (Arzner & Scholer, 2001; Karimabadi et al., 1999; Palmroth et al., 2023). In particular, the hybrid simulations of Arzner and Scholer (2001) demonstrated that the passage of a plasmoid or flux rope can create a post-plasmoid/flux rope CS populated by anisotropic, non-Maxwellian ion distributions. These conditions render the CS unstable, leading to flapping motions, filamentation, and turbulence in the CS. Importantly, the instabilities in their model convect tailward with the reconnection outflow, producing magnetic fluctuations and spectral features broadly consistent with spacecraft observations at Earth. This may provide a plausible mechanism by which reconnection-generated magnetic flux ropes may contribute to the CS flapping in the Martian magnetotail as observed in our study. While detailed kinetic simulations of these processes in the Martian magnetotail remain lacking to confirm such mechanism, a previous study by Ma et al. (2018) employed an MHD model with embedded particle-in-cell simulations in the Martian magnetotail, successfully reproducing the onset of magnetic reconnection and the formation of magnetic flux ropes during reconnection, highlighting the potential capability of such models in simulating Martian magnetotail dynamics. Looking forward, dedicated kinetic simulations will be essential to clarify how magnetic reconnection may affect both the upstream and downstream regions of the Martian magnetotail in the future study.

Despite the insights from previous studies and the evidence presented in our observations, the statistical survey also showed that roughly one-third of the flapping events detected by TW-1 exhibited no clear reconnection signatures in MAVEN data. This may reflect either observational limitations, as MAVEN's trajectory may not always be able to observe the reconnection site or diffusion regions associated with the downstream flapping, or it

may also imply that additional mechanisms can trigger the tail flapping at Mars. Possible candidates previously discussed in DiBraccio et al. (2017) include solar wind pertubations (C. Shen et al., 2008; G. Wang et al., 2019), penetration of Alfvénic waves (Romanelli et al., 2024; Ruhunusiri et al., 2015) into the tail, or the Kelvin–Helmholtz instability (Poh et al., 2021; Ruhunusiri et al., 2016). However, none of these proposed triggering mechanisms have been observationally verified at Mars to date. As an additional assessment, we attempted to explore the feasibility of the magnetic double-gradient instability (MDGI) at Mars, which has been proposed as a driver of kink-like CS flapping in Earth's magnetotail (Erkaev et al., 2007, 2008). Using a data-constrained, multi-year averaged Martian magnetotail magnetic field model derived from MAVEN observations, we evaluated the MDGI instability criterion based on the product of orthogonal magnetic field gradients and compared the characteristic flapping period predicted by the MDGI model with observed flapping periods at Mars. The results of this analysis, presented in Supporting Information S1, indicate that the MDGI criterion is not systematically satisfied near the central Martian magnetotail CS under average conditions, and that the characteristic periods predicted by the model are substantially different from the flapping periods typically observed by MAVEN (C. Zhang et al., 2023). These findings suggest that, while MDGI may not be completely ruled out as a localized or transient contributor, it may not be the dominant mechanism responsible for the kink-like flapping observed in the Martian magnetotail. This comparison between theory and observations may also reflect fundamental differences in magnetic field structure and plasma conditions between induced magnetosphere like Mars and intrinsic magnetospheres such as Earth's. A more definitive assessment of the MDGI role at Mars may require dedicated analytical modeling and fully kinetic or hybrid numerical simulations tailored to the induced magnetospheric environment in the future study.

In addition, open questions still remain regarding the nature of the observed flapping in our study, given current observational limitations. For example, it is not possible to determine whether reconnection-associated flapping is a localized process confined to certain regions of the tail or a large-scale global phenomenon affecting the entire downstream magnetotail, nor how long flapping motions triggered by reconnection may persist. If such reconnection-associated flux ropes also propagate planetward and trigger upstream tail flapping, it may produce observable consequences near Mars, potentially including oscillatory or sinuous auroral structures as those recently reported in Martian auroral observations (Lillis et al., 2024). Addressing these questions will likely require coordinated measurements spanning different regions of the Martian magnetotail, together with simultaneous auroral imaging, which is challenging to achieve.

5. Conclusions

In summary, based on the analysis of an example event and a statistical survey of MAVEN and TW-1 joint observations, we find evidence for a statistically significant association between magnetic reconnection in the upstream tail and CS flapping in the downstream Martian magnetotail. Building on insights from analogous processes observed at Earth and observational evidence in our study, we proposed a potential mechanism that reconnection-generated magnetic flux ropes may propagate tailward, altering the plasma environment and driving plasma instabilities that give rise to flapping motions observed in the downstream magnetotail. However, it is important to emphasize that even at Earth, despite the availability of high-resolution, multi-spacecraft missions such as Cluster, THEMIS, and MMS, establishing a definitive causal relationship between reconnection and tail flapping based solely on in situ observations remains challenging at this stage, interlinked dynamics between reconnection and flapping continue to be an active topic of research (Hwang et al., 2026).

This study provides valuable insights into the statistical intercorrelation between reconnection and tail flapping at Mars, and the potential triggering mechanism of the magnetotail CS flapping beyond the terrestrial magnetosphere for the first time. While these findings demonstrate that reconnection may play an important role in triggering tail flapping, the absence of reconnection signatures in a fraction of our events indicates that other mechanisms may also contribute (e.g., solar wind perturbations). Future multipoint observations and dedicated kinetic simulations in the Martian magnetotail will therefore be essential to disentangle the relative roles of reconnection and alternative drivers in controlling the dynamics of the Martian magnetotail. With the continued operations of MAVEN and TW-1, together with the upcoming ESCAPADE (Lillis et al., 2022) and MMX missions (Matsuoka et al., 2025), an abundance of joint observations will soon become available in the near future, offering a unique opportunity to substantially advance our understanding of plasma dynamics in the Martian magnetotail.

Conflict of Interest

The authors declare no conflicts of interest relevant to this study.

Availability Statement

The research described in this study utilizes publicly available data from the MAVEN Science Data Center (https://lasp.colorado.edu/maven/sdc/public/data/sci/) and NASA Planetary Data System (https://pds-ppi.igpp.ucla.edu/), including data from the MAG (Connerney, 2024), STATIC (J. P. McFadden, 2024), SWIA (J. S. Halekas, 2024), SWEA (D. L. Mitchell, 2024) instruments. The Tianwen-1 MOMAG data are publicly available at the Lunar and Planetary Data Release System (https://moon.bao.ac.cn/) and the MOMAG official website (https://space.ustc.edu.cn/dreams/tw1_momag/).

Acknowledgments

Y. Wen acknowledges Prof. Zhaojin Rong, Dr. Takuya Hara, Prof. Ivan Vasko, Dr. Andrei Runov, Dr. Weijie Sun, Dr. Jacob R. Gruesbeck, Murti Nauth, and Kyle Webster for helpful discussions on this study. We acknowledge NASA and the MAVEN mission for support through grant NNH10CC04C to the University of Colorado and by subcontract to Space Sciences Laboratory, University of California, Berkeley. N. Romanelli is supported by NASA under award number 80GSFC24M0006. We also acknowledge the Tianwen-1 MOMAG team for providing public data access and support. Part of this work is supported by the French space agency CNES for the observations obtained with the SWEA instrument.

References

Acuna, M. H., Connerney, J. E. P., Ness, N. F., Lin, R. P., Mitchell, D., Carlson, C. W., et al. (1999). Global distribution of crustal magnetization discovered by the Mars Global Surveyor MAG/ER experiment. *Science*, *284*(5415), 790–793. https://doi.org/10.1126/science.284.5415.790

Arzner, K., & Scholer, M. (2001). Kinetic structure of the post plasmoid plasma sheet during magnetotail reconnection. *Journal of Geophysical Research*, *106*(A3), 3827–3844. https://doi.org/10.1029/2000ja000179

Azari, A., Abrahams, E., Sapienza, F., Mitchell, D., Biersteker, J., Xu, S., et al. (2023). Magnetic field draping in induced magnetospheres: Evidence from the MAVEN mission to Mars. *Journal of Geophysical Research: Space Physics*, *128*(11), e2023JA031546. https://doi.org/10.1029/2023JA031546

Barabash, S., Fedorov, A., Lundin, R., & Sauvaud, J.-A. (2007). Martian atmospheric erosion rates. *Science*, *315*(5811), 501–503. https://doi.org/10.1126/science.1134358

Barabash, S., Holmström, M., Ramstad, R., Futaana, Y., & Voshchepynets, A. (2025). The induced magnetosphere of Mars and the near-Mars environment as revealed by Mars Express. *Space Science Reviews*, *221*(6), 79. https://doi.org/10.1007/s11214-025-01206-1

Bertucci, C., Duru, F., Edberg, N., Fraenz, M., Martinecz, C., Szego, K., & Vaisberg, O. (2011). The induced magnetospheres of Mars, Venus, and Titan. *Space Science Reviews*, *162*(1–4), 113–171. https://doi.org/10.1007/s11214-011-9845-1

Brain, D., Bagenal, F., Acuña, M., & Connerney, J. (2003). Martian magnetic morphology: Contributions from the solar wind and crust. *Journal of Geophysical Research*, *108*(A12), 1424. https://doi.org/10.1029/2002JA009482

Brain, D., Lillis, R., Mitchell, D., Halekas, J., & Lin, R. (2007). Electron pitch angle distributions as indicators of magnetic field topology near Mars. *Journal of Geophysical Research*, *112*(A9), A09201. https://doi.org/10.1029/2007JA012435

Cheng, L., Lillis, R., Wang, Y., Mittelholz, A., Xu, S., Mitchell, D. L., et al. (2023). Martian bow shock oscillations driven by solar wind variations: Simultaneous observations from Tianwen-1 and MAVEN. *Geophysical Research Letters*, *50*(16), e2023GL104769. https://doi.org/10.1029/2023gl104769

Cheng, L., Wang, Y., Lillis, R., Halekas, J., Langlais, B., Zhang, T., et al. (2024). Two-spacecraft observations of asymmetric Martian bow shock: Conjunctions of Tianwen-1 and MAVEN. *Journal of Geophysical Research: Space Physics*, *129*(9), e2024JA033185. https://doi.org/10.1029/2024ja033185

Cheng, L., Wang, Y., Ma, Y., Lillis, R., Halekas, J., Langlais, B., et al. (2025). Bow shock oscillations of Mars under weakly disturbed solar wind conditions. *Nature Communications*, *16*(1), 9649. https://doi.org/10.1038/s41467-025-65011-8

Connerney, J. E. P. (2024). NASA Planetary Data System. Retrieved from https://pds-ppi.igpp.ucla.edu/collection/urn:nasa:pds:maven.mag.calibrated:data.ss

Connerney, J. E. P., Espley, J., Lawton, P., Murphy, S., Odom, J., Oliversen, R., & Sheppard, D. (2015). The MAVEN magnetic field investigation. *Space Science Reviews*, *195*(1), 257–291. https://doi.org/10.1007/s11214-015-0169-4

De Hoffmann, F., & Teller, E. (1950). Magneto-hydrodynamic shocks. *Physical Review*, *80*(4), 692–703. https://doi.org/10.1103/PhysRev.80.692

DiBraccio, G. A., Dann, J., Espley, J. R., Gruesbeck, J. R., Soobiah, Y., Connerney, J. E., et al. (2017). Maven observations of tail current sheet flapping at Mars. *Journal of Geophysical Research: Space Physics*, *122*(4), 4308–4324. https://doi.org/10.1002/2016JA023488

DiBraccio, G. A., Espley, J. R., Gruesbeck, J. R., Connerney, J. E., Brain, D. A., Halekas, J. S., et al. (2015). Magnetotail dynamics at Mars: Initial MAVEN observations. *Geophysical Research Letters*, *42*(21), 8828–8837. https://doi.org/10.1002/2015GL065248

DiBraccio, G. A., Luhmann, J. G., Curry, S. M., Espley, J. R., Xu, S., Mitchell, D. L., et al. (2018). The twisted configuration of the Martian magnetotail: MAVEN observations. *Geophysical Research Letters*, *45*(10), 4559–4568. https://doi.org/10.1029/2018GL077251

DiBraccio, G. A., Romanelli, N., Bowers, C. F., Gruesbeck, J. R., Halekas, J. S., Ruhunusiri, S., et al. (2022). A statistical investigation of factors influencing the magnetotail twist at Mars. *Geophysical Research Letters*, *49*(12), e2022GL098007. https://doi.org/10.1029/2022GL098007

Dong, Y., Fang, X., Brain, D., McFadden, J., Halekas, J., Connerney, J., et al. (2015). Strong plume fluxes at Mars observed by MAVEN: An important planetary ion escape channel. *Geophysical Research Letters*, *42*(21), 8942–8950. https://doi.org/10.1002/2015GL065346

Dong, Y., Fang, X., Brain, D., McFadden, J., Halekas, J., Connerney, J., et al. (2017). Seasonal variability of Martian ion escape through the plume and tail from MAVEN observations. *Journal of Geophysical Research: Space Physics*, *122*(4), 4009–4022. https://doi.org/10.1002/2016JA023517

Dubinin, E., & Fraenz, M. (2015). Magnetotails of Mars and Venus. *Magnetotails in the Solar System*, 43–59. https://doi.org/10.1002/9781118842324.ch3

Dubinin, E., Fraenz, M., Pätzold, M., Tellmann, S., Modolo, R., DiBraccio, G., et al. (2023). Magnetic fields and plasma motions in a hybrid Martian magnetosphere. *Journal of Geophysical Research: Space Physics*, *128*(1), e2022JA030575. https://doi.org/10.1029/2022JA030575

Dubinin, E., Fraenz, M., Woch, J., Zhang, T., Wei, J., Fedorov, A., et al. (2012). Bursty escape fluxes in plasma sheets of Mars and Venus. *Geophysical Research Letters*, *39*(1), L01104. https://doi.org/10.1029/2011GL049883

Eastwood, J., Brain, D., Halekas, J., Drake, J., Phan, T., Øieroset, M., et al. (2008). Evidence for collisionless magnetic reconnection at Mars. *Geophysical Research Letters*, *35*(2), L02106. https://doi.org/10.1029/2007GL032289

Eastwood, J., & Kiehas, S. (2015). Origin and evolution of plasmoids and flux ropes in the magnetotails of Earth and Mars. *Magnetotails in the Solar System*, 269–287.

Eastwood, J., Videira, J., Brain, D., & Halekas, J. (2012). A chain of magnetic flux ropes in the magnetotail of Mars. *Geophysical Research Letters*, *39*(3), L03104. https://doi.org/10.1029/2011gl050444

Erkaev, N., Semenov, V., & Biernat, H. (2007). Magnetic double-gradient instability and flapping waves in a current sheet. *Physical Review Letters*, *99*(23), 235003. https://doi.org/10.1103/physrevlett.99.235003

Erkaev, N., Semenov, V., & Biernat, H. (2008). Magnetic double gradient mechanism for flapping oscillations of a current sheet. *Geophysical Research Letters*, *35*(2), L02111. https://doi.org/10.1029/2007gl032277

Forsyth, C., Lester, M., Fear, R., Lucek, E., Dandouras, I., Fazakerley, A., et al. (2009). Solar wind and substorm excitation of the wavy current sheet. *Annales Geophysicae*, *27*(6), 2457–2474. https://doi.org/10.5194/angeo-27-2457-2009

Fowler, C., McFadden, J., Hanley, K., Mitchell, D., Curry, S., & Jakosky, B. (2022). In-situ measurements of ion density in the Martian ionosphere: Underlying structure and variability observed by the MAVEN-STATIC instrument. *Journal of Geophysical Research: Space Physics*, *127*(8), e2022JA030352. https://doi.org/10.1029/2022JA030352

Gabrielse, C., Angelopoulos, V., Runov, A., Kepko, L., Glassmeier, K., Auster, H., et al. (2008). Propagation characteristics of plasma sheet oscillations during a small storm. *Geophysical Research Letters*, *35*(17), L17S13. https://doi.org/10.1029/2008gl033664

Gao, J., Rong, Z., Cai, Y., Lui, A., Petrukovich, A., Shen, C., et al. (2018). The distribution of two flapping types of magnetotail current sheet: Implication for the flapping mechanism. *Journal of Geophysical Research: Space Physics*, *123*(9), 7413–7423. https://doi.org/10.1029/2018ja025695

Gao, J., Rong, Z., Persson, M., Stenberg, G., Zhang, Y., Klinger, L., et al. (2021). In situ observations of the ion diffusion region in the Venusian Magnetotail. *Journal of Geophysical Research: Space Physics*, *126*(1), e2020JA028547. https://doi.org/10.1029/2020ja028547

Greenwood, P. E., & Nikulin, M. S. (1996). *A guide to chi-squared testing*. John Wiley & Sons.

Guo, R., Yao, Z., Wei, Y., Ray, L., Rae, I., Arridge, C., et al. (2018). Rotationally driven magnetic reconnection in Saturn's dayside. *Nature Astronomy*, *2*(8), 640–645. https://doi.org/10.1038/s41550-018-0461-9

Halekas, J., Brain, D., Lillis, R., Fillingim, M., Mitchell, D., & Lin, R. (2006). Current sheets at low altitudes in the Martian magnetotail. *Geophysical Research Letters*, *33*(13), L13101. https://doi.org/10.1029/2006GL026229

Halekas, J., Eastwood, J., Brain, D., Phan, T., Øieroset, M., & Lin, R. (2009). In situ observations of reconnection hall magnetic fields at Mars: Evidence for ion diffusion region encounters. *Journal of Geophysical Research*, *114*(A11), A11204. https://doi.org/10.1029/2009JA014544

Halekas, J., Ruhunusiri, S., Harada, Y., Collinson, G., Mitchell, D., Mazelle, C., et al. (2017). Structure, dynamics, and seasonal variability of the Mars-solar wind interaction: MAVEN solar wind ion analyzer in-flight performance and science results. *Journal of Geophysical Research: Space Physics*, *122*(1), 547–578. https://doi.org/10.1002/2016JA023167

Halekas, J., Taylor, E., Dalton, G., Johnson, G., Curtis, D., McFadden, J., et al. (2015). The solar wind ion analyzer for MAVEN. *Space Science Reviews*, *195*(1–4), 125–151. https://doi.org/10.1007/s11214-013-0029-z

Halekas, J. S. (2024). NASA Planetary Data System. Retrieved from https://pds-ppi.igpp.ucla.edu/collection/urn:nasa:pds:maven.swia.calibrated:data.coarse_svy_3d

Halekas, J. S., Luhmann, J. G., Dubinin, E., & Ma, Y. (2021). Induced magnetospheres: Mars. *Magnetospheres in the Solar System*, 391–406. https://doi.org/10.1002/9781119815624.ch25

Hara, T., Harada, Y., Mitchell, D. L., DiBraccio, G. A., Espley, J. R., Brain, D. A., et al. (2017). On the origins of magnetic flux ropes in near-Mars magnetotail current sheets. *Geophysical Research Letters*, *44*(15), 7653–7662. https://doi.org/10.1002/2017gl073754

Hara, T., Huang, Z., Mitchell, D. L., DiBraccio, G. A., Brain, D. A., Harada, Y., & Luhmann, J. G. (2022). A comparative study of magnetic flux ropes in the nightside induced magnetosphere of Mars and Venus. *Journal of Geophysical Research: Space Physics*, *127*(1), e2021JA029867. https://doi.org/10.1029/2021ja029867

Hara, T., Mitchell, D. L., McFadden, J. P., Seki, K., Brain, D. A., Halekas, J. S., et al. (2015). Estimation of the spatial structure of a detached magnetic flux rope at Mars based on simultaneous MAVEN plasma and magnetic field observations. *Geophysical Research Letters*, *42*(21), 8933–8941. https://doi.org/10.1002/2015gl065720

Harada, Y., Halekas, J., McFadden, J., Espley, J., DiBraccio, G., Mitchell, D., et al. (2017). Survey of magnetic reconnection signatures in the Martian magnetotail with MAVEN. *Journal of Geophysical Research: Space Physics*, *122*(5), 5114–5131. https://doi.org/10.1002/2017JA023952

Harada, Y., Halekas, J., McFadden, J., Mitchell, D., Mazelle, C., Connerney, J., et al. (2015a). Magnetic reconnection in the near-Mars magnetotail: MAVEN observations. *Geophysical Research Letters*, *42*(21), 8838–8845. https://doi.org/10.1002/2015GL065004

Harada, Y., Halekas, J., McFadden, J., Mitchell, D., Mazelle, C., Connerney, J., et al. (2015b). Marsward and tailward ions in the near-Mars magnetotail: MAVEN observations. *Geophysical Research Letters*, *42*(21), 8925–8932. https://doi.org/10.1002/2015gl065005

Harada, Y., Halekas, J., Xu, S., DiBraccio, G., Ruhunusiri, S., Hara, T., et al. (2020). Ion jets within current sheets in the Martian magnetosphere. *Journal of Geophysical Research: Space Physics*, *125*(12), e2020JA028576. https://doi.org/10.1029/2020ja028576

Hwang, K.-J., Dokgo, K., Choi, E., Burch, J., Bessho, N., Hasegawa, H., et al. (2026). Causal relationship between current sheet flapping, electron-only reconnection, and ion-coupled reconnection. *The Astrophysical Journal*, *998*(1), 17. https://doi.org/10.3847/1538-4357/ae3536

Inui, S., Seki, K., Sakai, S., Brain, D., Hara, T., McFadden, J., et al. (2019). Statistical study of heavy ion outflows from Mars observed in the Martian-induced magnetotail by MAVEN. *Journal of Geophysical Research: Space Physics*, *124*(7), 5482–5497. https://doi.org/10.1029/2018JA026452

Jakosky, B. M., Lin, R. P., Grebowsky, J. M., Luhmann, J. G., Mitchell, D., Beutelschies, G., et al. (2015). The Mars Atmosphere and Volatile Evolution (MAVEN) Mission. *Space Science Reviews*, *195*(1–4), 3–48. https://doi.org/10.1007/s11214-015-0139-x

Karimabadi, H., Daughton, W., Pritchett, P., & Krauss-Varban, D. (2003). Ion-ion kink instability in the magnetotail: 1. Linear theory. *Journal of Geophysical Research*, *108*(A11), 1400. https://doi.org/10.1029/2003ja010026

Karimabadi, H., Krauss-Varban, D., Omidi, N., & Vu, H. (1999). Magnetic structure of the reconnection layer and core field generation in plasmoids. *Journal of Geophysical Research*, *104*(A6), 12313–12326. https://doi.org/10.1029/1999ja900089

Khrabrov, A. V., & Sonnerup, B. U. (1998). deHoffmann-Teller analysis. *ISSI Scientific Reports Series*, *1*, 221–248.

Li, X., Rong, Z., Fraenz, M., Zhang, C., Klinger, L., Shi, Z., et al. (2023). Two types of Martian magnetotail current sheets: MAVEN observations of ion composition. *Geophysical Research Letters*, *50*(2), e2022GL102630. https://doi.org/10.1029/2022GL102630

Liemohn, M. W., & Xu, S. (2018). Recent advances regarding the Mars magnetotail current sheet. *Electric Currents in Geospace and Beyond*, 177–190. https://doi.org/10.1002/9781119324522.ch11

Lillis, R. J., Curry, S., Ma, Y., Curtis, D., Taylor, E., Parker, J., et al. (2022). ESCAPADE: A twin-spacecraft SIMPLEX mission to unveil Mars' unique hybrid magnetosphere. *Low-Cost Science Mission Concepts for Mars Exploration*, *2655*, 5012.

Lillis, R. J., Deighan, J., Chirakkil, K., Jain, S., Fillingim, M., Chaffin, M., et al. (2024). Sinuous aurora at Mars: A link to the tail current sheet? *Journal of Geophysical Research: Space Physics*, *129*(6), e2024JA032477. https://doi.org/10.1029/2024ja032477

Liu, Y., Mouikis, C., Kistler, L., Wang, S., Roytershteyn, V., & Karimabadi, H. (2015). The heavy ion diffusion region in magnetic reconnection in the Earth's magnetotail. *Journal of Geophysical Research: Space Physics*, *120*(5), 3535–3551. https://doi.org/10.1002/2015JA020982

Ma, Y., Fang, X., Russell, C. T., Nagy, A. F., Toth, G., Luhmann, J. G., et al. (2014). Effects of crustal field rotation on the solar wind plasma interaction with Mars. *Geophysical Research Letters*, *41*(19), 6563–6569. https://doi.org/10.1002/2014gl060785

Ma, Y., Russell, C. T., Toth, G., Chen, Y., Nagy, A. F., Harada, Y., et al. (2018). Reconnection in the Martian magnetotail: Hall-MHD with embedded particle-in-cell simulations. *Journal of Geophysical Research: Space Physics*, *123*(5), 3742–3763. https://doi.org/10.1029/2017ja024729

Matsuoka, A., Yokota, S., Murata, N., Harada, Y., Imajo, S., Terada, N., et al. (2025). Magnetic field experiment at Phobos and in space around Mars by the Martian Moons eXploration (MMX) mission. *Progress in Earth and Planetary Science*, *12*(1), 67. https://doi.org/10.1186/s40645-025-00738-y

McFadden, J., Kortmann, O., Curtis, D., Dalton, G., Johnson, G., Abiad, R., et al. (2015). MAVEN SupraThermal And Thermal Ion Compostion (STATIC) instrument. *Space Science Reviews*, *195*(1–4), 199–256. https://doi.org/10.1007/s11214-015-0175-6

McFadden, J. P. (2024). NASA Planetary Data System. Retrieved from https://pds-ppi.igpp.ucla.edu/collection/urn:nasa:pds:maven.static.c:data.d0_32e4d16a8m

Mitchell, D., Mazelle, C., Sauvaud, J.-A., Thocaven, J.-J., Rouzaud, J., Fedorov, A., et al. (2016). The MAVEN solar wind electron analyzer. *Space Science Reviews*, *200*(1–4), 495–528. https://doi.org/10.1007/s11214-015-0232-1

Mitchell, D. L. (2024). NASA Planetary Data System. Retrieved from https://pds-ppi.igpp.ucla.edu/collection/urn:nasa:pds:maven.swea.calibrated:data.svy_3d

Nagy, A., Winterhalter, D., Sauer, K., Cravens, T., Brecht, S., Mazelle, C., et al. (2004). The plasma environment of Mars. *Space Science Reviews*, *111*(1–2), 33–114. https://doi.org/10.1023/B:SPAC.0000032718.47512.92

Nakagawa, T., & Nishida, A. (1989). Southward magnetic field in the neutral sheet produced by wavy motions propagating in the dawn-dusk direction. *Geophysical Research Letters*, *16*(11), 1265–1268. https://doi.org/10.1029/gl016i011p01265

Nilsson, H., Carlsson, E., Brain, D. A., Yamauchi, M., Holmström, M., Barabash, S., et al. (2010). Ion escape from Mars as a function of solar wind conditions: A statistical study. *Icarus*, *206*(1), 40–49. https://doi.org/10.1016/j.icarus.2009.03.006

Nilsson, H., Zhang, Q., Wieser, G. S., Holmström, M., Barabash, S., Futaana, Y., et al. (2023). Solar cycle variation of ion escape from Mars. *Icarus*, *393*, 114610. https://doi.org/10.1016/j.icarus.2021.114610

Øieroset, M., Phan, T. D., Lin, R. P., & Sonnerup, B. U. (2000). Walén and variance analyses of high-speed flows observed by Wind in the midtail plasma sheet: Evidence for reconnection. *Journal of Geophysical Research*, *105*(A11), 25247–25263. https://doi.org/10.1029/2000ja900075

Palmroth, M., Pulkkinen, T. I., Ganse, U., Pfau-Kempf, Y., Koskela, T., Zaitsev, I., et al. (2023). Magnetotail plasma eruptions driven by magnetic reconnection and kinetic instabilities. *Nature Geoscience*, *16*(7), 570–576. https://doi.org/10.1038/s41561-023-01206-2

Parker, E. N. (1957). Sweet's mechanism for merging magnetic fields in conducting fluids. *Journal of Geophysical Research*, *62*(4), 509–520. https://doi.org/10.1029/jz062i004p00509

Paschmann, G., & Sonnerup, B. U. (2008). Proper frame determination and Walen test. *ISSI Scientific Reports Series*, *8*, 65–74.

Petrenko, B., Kozak, L., Kronberg, E., & Akhmetshyn, R. (2023). Multispacecraft wave analysis of current sheet flapping motions in Earth's magnetotail. *Frontiers in Astronomy and Space Sciences*, *9*, 1071824. https://doi.org/10.3389/fspas.2022.1071824

Phan, T., Dunlop, M., Paschmann, G., Klecker, B., Bosqued, J., Reme, H., et al. (2004). Cluster observations of continuous reconnection at the magnetopause under steady interplanetary magnetic field conditions. *Annales Geophysicae*, *22*(7), 2355–2367. https://doi.org/10.5194/angeo-22-2355-2004

Poh, G., Espley, J. R., Nykyri, K., Fowler, C. M., Ma, X., Xu, S., et al. (2021). On the growth and development of non-linear Kelvin–Helmholtz instability at Mars: MAVEN observations. *Journal of Geophysical Research: Space Physics*, *126*(9), e2021JA029224. https://doi.org/10.1029/2021JA029224

Poh, G., Sun, W., Clink, K. M., Slavin, J. A., Dewey, R. M., Jia, X., et al. (2020). Large-amplitude oscillatory motion of Mercury's cross-tail current sheet. *Journal of Geophysical Research: Space Physics*, *125*(7), e2020JA027783. https://doi.org/10.1029/2020ja027783

Romanelli, N., Fowler, C. M., DiBraccio, G. A., Espley, J. R., & Halekas, J. S. (2024). Alfvén waves at Mars. *Alfvén Waves Across Heliophysics: Progress, Challenges, and Opportunities*, 99–123.

Rong, Z., Barabash, S., Stenberg, G., Futaana, Y., Zhang, T., Wan, W., et al. (2015a). The flapping motion of the Venusian magnetotail: Venus express observations. *Journal of Geophysical Research: Space Physics*, *120*(7), 5593–5602. https://doi.org/10.1002/2015JA021317

Rong, Z., Barabash, S., Stenberg, G., Futaana, Y., Zhang, T., Wan, W., et al. (2015b). Technique for diagnosing the flapping motion of magnetotail current sheets based on single-point magnetic field analysis. *Journal of Geophysical Research: Space Physics*, *120*(5), 3462–3474. https://doi.org/10.1002/2014JA020973

Rong, Z., Shen, C., Petrukovich, A., Wan, W., & Liu, Z. (2010). The analytic properties of the flapping current sheets in the Earth magnetotail. *Planetary and Space Science*, *58*(10), 1215–1229. https://doi.org/10.1016/j.pss.2010.04.016

Rong, Z., Zhang, C., Klinger, L., Shen, C., Cui, J., Zhang, Y., & Wei, Y. (2021). A single-point method to quantitatively diagnose the magnetotail flapping motion. *Journal of Geophysical Research: Space Physics*, *126*(2), e2020JA028200. https://doi.org/10.1029/2020ja028200

Ruhunusiri, S., Halekas, J., Connerney, J., Espley, J., McFadden, J., Larson, D., et al. (2015). Low-frequency waves in the Martian magnetosphere and their response to upstream solar wind driving conditions. *Geophysical Research Letters*, *42*(21), 8917–8924. https://doi.org/10.1002/2015gl064968

Ruhunusiri, S., Halekas, J., McFadden, J., Connerney, J., Espley, J., Harada, Y., et al. (2016). Maven observations of partially developed Kelvin-Helmholtz vortices at Mars. *Geophysical Research Letters*, *43*(10), 4763–4773. https://doi.org/10.1002/2016gl068926

Runov, A., Angelopoulos, V., Sergeev, V., Glassmeier, K.-H., Auster, U., McFadden, J., et al. (2009). Global properties of magnetotail current sheet flapping: THEMIS perspectives. *Annales Geophysicae*, *27*(1), 319–328. https://doi.org/10.5194/angeo-27-319-2009

Russell, C. T., & Elphic, R. (1979). Observation of magnetic flux ropes in the Venus ionosphere. *Nature*, *279*(5714), 616–618. https://doi.org/10.1038/279616a0

Sánchez-Cano, B., Lester, M., Andrews, D. J., Opgenoorth, H., Lillis, R., Leblanc, F., et al. (2022). Mars' plasma system. Scientific potential of coordinated multipoint missions: "The next generation". *Experimental Astronomy*, *54*(2), 641–676. https://doi.org/10.1007/s10686-021-09790-0

Sergeev, V., Angelopoulos, V., Carlson, C., & Sutcliffe, P. (1998). Current sheet measurements within a flapping plasma sheet. *Journal of Geophysical Research*, *103*(A5), 9177–9187. https://doi.org/10.1029/97ja02093

Sergeev, V., Runov, A., Baumjohann, W., Nakamura, R., Zhang, T., Balogh, A., et al. (2004). Orientation and propagation of current sheet oscillations. *Geophysical Research Letters*, *31*(5), L05807. https://doi.org/10.1029/2003gl019346

Sergeev, V., Sormakov, D., Apatenkov, S., Baumjohann, W., Nakamura, R., Runov, A., et al. (2006). Survey of large-amplitude flapping motions in the midtail current sheet. *Annales Geophysicae*, *24*(7), 2015–2024. https://doi.org/10.5194/angeo-24-2015-2006

Sergeev, V., Tsyganenko, N., & Angelopoulos, V. (2008). Dynamical response of the magnetotail to changes of the solar wind direction: An MHD modeling perspective. *Annales Geophysicae*, *26*(8), 2395–2402. https://doi.org/10.5194/angeo-26-2395-2008

Shen, C., Rong, Z., Li, X., Dunlop, M., Liu, Z., Malova, H., et al. (2008). Magnetic configurations of the tilted current sheets in magnetotail. *Annales Geophysicae*, *26*(11), 3525–3543. https://doi.org/10.5194/angeo-26-3525-2008

Shen, H.-W., Halekas, J. S., Curry, S. M., Zhang, C., Wen, Y., & Espley, J. R. (2025). Statistical analysis of ion properties in the Martian magnetosheath based on MAVEN observations: A comparison of core and total ion populations. *The Astrophysical Journal*, *990*(2), 115. https://doi.org/10.3847/1538-4357/adf6a9

Shen, H.-W., Halekas, J. S., McFadden, J. P., Gruesbeck, J. R., & Schnepf, N. R. (2024). Heavy ion escape at Mars during the disappearing solar wind event in 2022 December. *The Astrophysical Journal*, *975*(2), 175. https://doi.org/10.3847/1538-4357/ad84f6

Shen, H.-W., Halekas, J. S., Xu, S., Shue, J.-H., Wen, Y., Zhang, C., et al. (2026). Strongly sub-isothermal polytropic behavior of ions in the martian magnetosheath revealed by MAVEN observations. *The Astrophysical Journal*. https://doi.org/10.3847/1538-4357/ae5a91

Sitnov, M., Birn, J., Ferdousi, B., Gordeev, E., Khotyaintsev, Y., Merkin, V., et al. (2019). Explosive magnetotail activity. *Space Science Reviews*, *215*(4), 31. https://doi.org/10.1007/s11214-019-0599-5

Sitnov, M., Merkin, V., Swisdak, M., Motoba, T., Buzulukova, N., Moore, T., et al. (2014). Magnetic reconnection, buoyancy, and flapping motions in magnetotail explosions. *Journal of Geophysical Research: Space Physics*, *119*(9), 7151–7168. https://doi.org/10.1002/2014ja020205

Sonnerup, B. U. Ö. (1998). Minimum and maximum variance analysis. *Analysis Methods for Multi-Spacecraft Data*, *1*, 185.

Sonnerup, B. U. Ö., Papamastorakis, I., Paschmann, G., & Lühr, H. (1987). Magnetopause properties from AMPTE/IRM observations of the convection electric field: Method development. *Journal of Geophysical Research*, *92*(A11), 12137–12159. https://doi.org/10.1029/ja092ia11p12137

Speiser, T. W., & Ness, N. F. (1967). The neutral sheet in the geomagnetic tail: Its motion, equivalent currents, and field line connection through it. *Journal of Geophysical Research*, *72*(1), 131–141. https://doi.org/10.1029/jz072i001p00131

Sweet, P. (1958). Electromagnetic phenomena in cosmical physics. In *IAU Symposium 6* (Vol. 123). Kluwer Academic Publishers.

Szegö, K., Glassmeier, K.-H., Bingham, R., Bogdanov, A., Fischer, C., Haerendel, G., et al. (2000). Physics of mass loaded plasmas. *Space Science Reviews*, *94*(3), 429–671. https://doi.org/10.1023/a:1026568530975

Tsutomu, T., & Teruki, M. (1976). Flapping motions of the tail plasma sheet induced by the interplanetary magnetic field variations. *Planetary and Space Science*, *24*(2), 147–159. https://doi.org/10.1016/0032-0633(76)90102-1

Vignes, D., Mazelle, C., Rme, H., Acuña, M., Connerney, J., Lin, R., et al. (2000). The solar wind interaction with Mars: Locations and shapes of the bow shock and the magnetic pile-up boundary from the observations of the MAG/ER Experiment onboard Mars Global Surveyor. *Geophysical Research Letters*, *27*(1), 49–52. https://doi.org/10.1029/1999GL010703

Volwerk, M., Andre, N., Arridge, C., Jackman, C., Jia, X., Milan, S. E., et al. (2013). Comparative magnetotail flapping: An overview of selected events at Earth, Jupiter and Saturn. *Annales Geophysicae*, *31*(5), 817–833. https://doi.org/10.5194/angeo-31-817-2013

Volwerk, M., Glassmeier, K.-H., Runov, A., Nakamura, R., Baumjohann, W., Klecker, B., et al. (2004). Flow burst–induced large-scale plasma sheet oscillation. *Journal of Geophysical Research*, *109*(A11), A11208. https://doi.org/10.1029/2004ja010533

Vörös, Z. (2011). Magnetic reconnection associated fluctuations in the deep magnetotail: ARTEMIS results. *Nonlinear Processes in Geophysics*, *18*(6), 861–869. https://doi.org/10.5194/npg-18-861-2011

Vörös, Z., Yordanova, E., Varsani, A., Genestreti, K., Khotyaintsev, Y. V., Li, W., et al. (2017). MMS observation of magnetic reconnection in the turbulent magnetosheath. *Journal of Geophysical Research: Space Physics*, *122*(11), 11–442. https://doi.org/10.1002/2017ja024535

Wang, G., Xiao, S., Wu, M., Zhao, Y., Jiang, S., Pan, Z., et al. (2024). Calibration of the zero offset of the fluxgate magnetometer on board the Tianwen-1 orbiter in the Martian magnetosheath. *Journal of Geophysical Research: Space Physics*, *129*(1), e2023JA031757. https://doi.org/10.1029/2023JA031757

Wang, G., Zhang, T., Wu, M., Schmid, D., Cao, J., & Volwerk, M. (2019). Solar wind directional change triggering flapping motions of the current sheet: MMS observations. *Geophysical Research Letters*, *46*(1), 64–70. https://doi.org/10.1029/2018gl080023

Wang, L., Huang, C., Du, A., Ge, Y., Chen, G., Fan, J., & Qin, J. (2023). Magnetic reconnection in the Martian magnetotail: Occurrence rate and impact on ion loss. *Geophysical Research Letters*, *50*(18), e2023GL104996. https://doi.org/10.1029/2023GL104996

Wang, L., Huang, C., Ge, Y., Du, A., Wang, R., Zhang, T., et al. (2022). Heavy ion escape from Martian wake enhanced by magnetic reconnection. *Journal of Geophysical Research: Planets*, *127*(6), e2022JE007181. https://doi.org/10.1029/2022JE007181

Wang, Y., Zhang, T., Wang, G., Xiao, S., Zou, Z., Cheng, L., et al. (2023). The Mars orbiter magnetometer of Tianwen-1: In-flight performance and first science results. *Earth and Planetary Physics*, *7*(2), 216–228. https://doi.org/10.26464/epp2023028

Wei, Y., Huang, S., Rong, Z., Yuan, Z., Jiang, K., Deng, X., et al. (2019). Observations of short-period current sheet flapping events in the Earth's magnetotail. *The Astrophysical Journal Letters*, *874*(2), L18. https://doi.org/10.3847/2041-8213/ab0f28

Wen, Y., Halekas, J. S., Shen, H.-W., Azari, A. R., Brain, D. A., Dong, Y., et al. (2025). Multipoint observations of magnetic reconnection in the Martian magnetotail triggered by an interplanetary magnetic field rotation. *The Astrophysical Journal Letters*, *982*(2), L42. https://doi.org/10.3847/2041-8213/adbf10

Wen, Y., Rong, Z., Nilsson, H., Zhang, C., Shen, H.-W., & Gao, J. (2025). Statistical investigations of the radial interplanetary magnetic field component impact on the magnetotail current sheet structure of Mars: MAVEN observations. *The Astrophysical Journal*, *993*(2), 201. https://doi.org/10.3847/1538-4357/ae11b3

Wu, M., Lu, Q., Volwerk, M., Vörös, Z., Ma, X., & Wang, S. (2016). Current sheet flapping motions in the tailward flow of magnetic reconnection. *Journal of Geophysical Research: Space Physics*, *121*(8), 7817–7827. https://doi.org/10.1002/2016ja022819

Xu, S., Huang, S., Yuan, Z., Jiang, K., Wu, H., Zhang, J., et al. (2025). Short-period flapping motion of current sheet in Saturn's magnetosphere. *Journal of Geophysical Research: Planets*, *130*(2), e2024JE008682. https://doi.org/10.1029/2024je008682

Zhang, C., Rong, Z., Gao, J., Zhong, J., Chai, L., Wei, Y., et al. (2020). The flapping motion of Mercury's magnetotail current sheet: Messenger observations. *Geophysical Research Letters*, *47*(4), e2019GL086011. https://doi.org/10.1029/2019gl086011

Zhang, C., Rong, Z., Klinger, L., Nilsson, H., Shi, Z., He, F., et al. (2022). Three-dimensional configuration of induced magnetic fields around Mars. *Journal of Geophysical Research: Planets*, *127*(8), e2022JE007334. https://doi.org/10.1029/2022JE007334

Zhang, C., Rong, Z., Li, X., Fränz, M., Nilsson, H., Jarvinen, R., et al. (2024). The energetic oxygen ion beams in the Martian magnetotail current sheets: Hints from the comparisons between two types of current sheets. *Geophysical Research Letters*, *51*(5), e2023GL107190. https://doi.org/10.1029/2023GL107190

Zhang, C., Rong, Z., Zhang, L., Gao, J., Shi, Z., Klinger, L., et al. (2023). Properties of flapping current sheet of the Martian magnetotail. *Journal of Geophysical Research: Space Physics*, *128*(4), e2022JA031232. https://doi.org/10.1029/2022JA031232

Zhang, T., Baumjohann, W., Nakamura, R., Balogh, A., & Glassmeier, K.-H. (2002). A wavy twisted neutral sheet observed by CLUSTER. *Geophysical Research Letters*, *29*(19), 5-1–5-4. https://doi.org/10.1029/2002gl015544

Zhang, T., Nakamura, R., Volwerk, M., Runov, A., Baumjohann, W., Eichelberger, H., et al. (2005). Double Star/Cluster observation of neutral sheet oscillations on 5 August 2004. *Annales Geophysicae*, *23*(8), 2909–2914. https://doi.org/10.5194/angeo-23-2909-2005

Zhang, Y. (2016). Distinct characteristics of asymmetric magnetic reconnections: Observational results from the exhaust region at the dayside magnetopause. *Scientific Reports*, *6*(1), 27592. https://doi.org/10.1038/srep27592

Zhang, Y., Dai, L., Rong, Z., Wang, C., Rème, H., Dandouras, I., et al. (2020). Observation of the large-amplitude and fast-damped plasma sheet flapping triggered by reconnection-induced ballooning instability. *Journal of Geophysical Research: Space Physics*, *125*(9), e2020JA028218. https://doi.org/10.1029/2020ja028218

Zou, Y., Zhu, Y., Bai, Y., Wang, L., Jia, Y., Shen, W., et al. (2021). Scientific objectives and payloads of Tianwen-1, China's first Mars exploration mission. *Advances in Space Research*, *67*(2), 812–823. https://doi.org/10.1016/j.asr.2020.11.005

Zou, Z., Wang, Y., Zhang, T., Wang, G., Xiao, S., Pan, Z., et al. (2023). In-flight calibration of the magnetometer on the Mars orbiter of Tianwen-1. *Science China Technological Sciences*, *66*(8), 2396–2405. https://doi.org/10.1007/s11431-023-2401-2

References From the Supporting Information

Dunlop, M. W., & Eastwood, J. P. (2008). The curlometer and other gradient based methods. *ISSI Scientific Reports Series*, *8*, 17–26.

Zhang, C., Dong, C., Zhou, H., Halekas, J., Li, X., Gao, J., et al. (2025). Global energy transport and conversion in the solar wind-Mars interaction: MAVEN observations. *Journal of Geophysical Research: Planets*, *130*(10), e2025JE009295. https://doi.org/10.1029/2025je009295